

Simulation of wind-related hazards avoidance when UAS operation in urban environment

Yuliya Averyanova^{1,†}, Maxim Ivanytskyi^{1,†}, Bohdan Shershen^{1,†}, Yevheniia Znakovska^{1,*†} and Yaryna Zhdanova^{2,†}

¹ National Aviation University, Liubomyra Huzara Ave., 1, Kyiv, 03058, Ukraine

² University of Vic-Central University of Catalonia, Ctra. de Roda, 70, Vic, 08500, Spain

Abstract

Nowadays unmanned aircraft systems (UASs) are planned to be used in many branches of people's activity and fulfill different tasks. Many of the tasks including cargo delivery, photo and filmmaking, future transportation, monitoring, different security applications, and others are, obviously the subject of urban flying. In this case, the different constraints should be taken into account. Some of the constraints are connected with weather-related hazards. In this paper, we consider the in-flight flight trajectory correction to avoid temporary dangerous areas for flight. We present a decision support system that can be used by remote pilots or implemented as a component of an onboard flight control system for hazard detection and operative conflict resolution. The system operation is based on information fusion from the network of distributed sensors additionally to the general set of data. The simulation of proposed trajectory corrections is shown and discussed. Also, we discuss the potential communication channels for operative information sharing and dissemination.

Keywords

air navigation, navigation, aviation, meteorology, UAS, simulation, trajectory correction, decision-making

1. Introduction

The prospects of drones utilizing in many branches of human activity and providing innovative aerial services [1] require consideration of a series of requirements [2] and restrictions to ensure the safe integration of unmanned aircraft system (UAS) into shared airspace [1, 3]. The concept of U-space as the area of airspace where UAS flights and operations are allowed [1, 3] considers the importance of the availability of information for all participants of air traffic. In [3] the outline of the common information services is shown. One of the requirements of the services is live operational data exchange to provide U-space

CMSE'24: International Workshop on Computational Methods in Systems Engineering, June 17, 2024, Kyiv, Ukraine

* Corresponding author.

† These authors contributed equally.

✉ ayua@nau.edu.ua (Yu. Averyanova); maksumiljano2002@gmail.com (M. Ivanytskyi); bogdansersen50@gmail.com (B. Shershen); zea@nau.edu.ua (Ye. Znakovska); yaryna.zhdanova@uvic.cat (Y. Zhdanova)

ORCID 0000-0002-9677-0805 (Yu. Averyanova); 0009-0007-0601-3901 (M. Ivanytskyi); 0000-0001-8572-1963 (B. Shershen); 0000-0002-9064-6256 (Ye. Znakovska); 0000-0002-9330-6679 (Y. Zhdanova)



© 2024 Copyright for this paper by its authors. Use permitted under Creative Commons License Attribution 4.0 International (CC BY 4.0).

services and ensure flight safety. Some of the factors that influence UAS flight safety are weather and weather-related phenomena. This can be especially important when flying over populated areas and in urban areas. Flying in urban areas is associated with additional unexpected and rapid weather-related hazards that are connected with higher irregularities of the underlying surface. These include buildings of different configurations and other constructions and their proximity, urban heat islands [4], and air pollutants. etc. In [5] it is mentioned that urban microclimates are the most complex and least understood. This is because of the heterogeneity of the constructions including industrial ones, other roughness elements, and the turbulence that can be present even under calm wind conditions and anthropogenic heat sources, in addition to other complex meteorological processes. Moreover, the climate change study [6] shows an increase in turbulence events over the globe. The weather-related risks for UAS are discussed in papers [7, 8, 9]. Paper [10] focuses also on the weather constraints for particular missions performed with UASs.

In this paper, we present the decision support system (DSS) that helps to evaluate weather-related risks when UAS flight planning. The system also can be used as a source of operative information for in-flight trajectory correction to avoid potentially hazardous regions. The simulation of the trajectory correction is presented and discussed. Also, the simulations to study the possibility of using ZigBee technology for information dissemination are presented and discussed. The presented system can be used by remote pilots or implemented as a component of an onboard flight control system for hazard detection and operative conflict resolution.

2. DSS overview and flight trajectory correction simulation

Decision-support systems (DSS) can be an important component of the air transportation subsystem [11], that considers the UASs operations, as they allow to collect and process the vast volumes of information and decrease the overload of the remote pilots.

In the paper [12] the general architecture of the DSS that collects, processes, and proposes the decisions based on the risk-oriented approach [13, 14] is presented. Different scenarios of remote pilot operations were simulated using the proposed system and results are presented and discussed in [15]. The automation in decision-making support with the developed system is discussed in [16]. The DSS operation can be depicted using the diagram shown in Figure 1.

Weather-related risks (Figure 1) are assessed by taking into account:

- Mission, as weather can significantly influence the ability to perform a particular task and has no influence on the general possibility of performing flight and other missions.
- The area of flight – urban or rural, over people assemble, etc. can be considered as an additional risky factor.
- Flight parameters can be connected with a particular mission as intended time, distance and with UAS characteristics.
- Additional apparatus placed at UAS to help in mission realization as they can be affected by weather.

- Information about current meteorological conditions and phenomena (used at the stage of preparation for the flight and mission).
- A type of unmanned aircraft and related characteristics.
- Data about current meteorological conditions and phenomena and dynamically changing weather conditions.

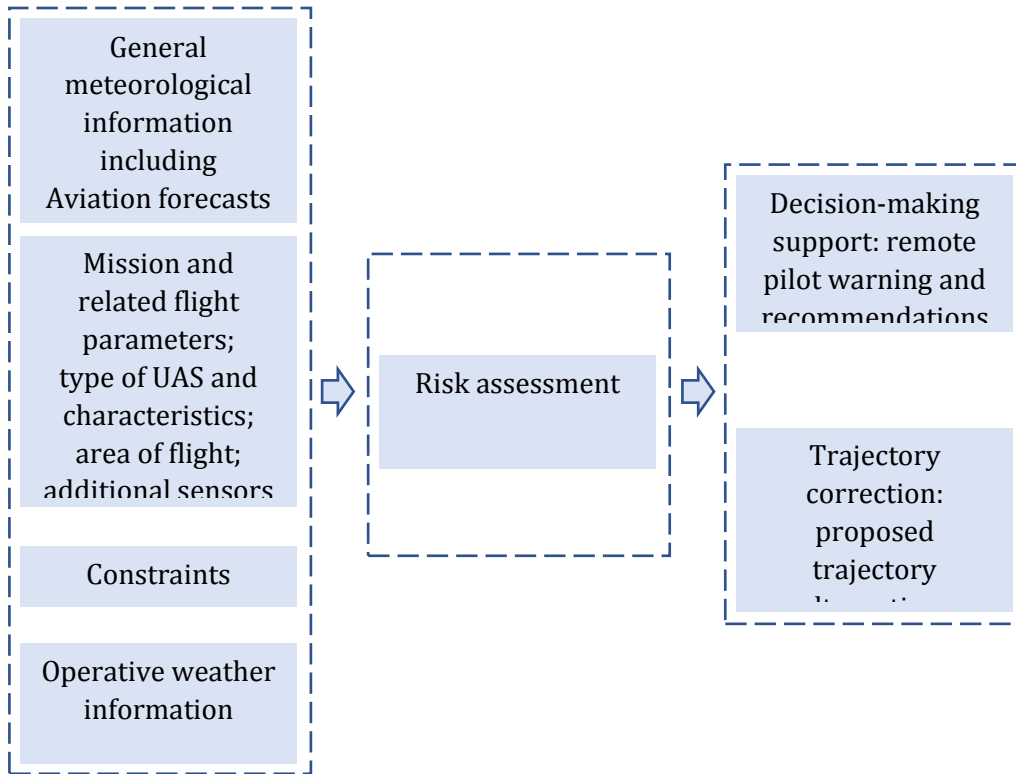


Figure 1: DSS general architecture.

The DSS can be used for automated flight trajectory correction (Figure 1). The important and remarkable feature of the system is that the fused information from the network of distributed and dynamic sensors is used to obtain operative information about weather hazards.

Results of UAS flight trajectory correction are presented in Figure 2. We considered the real meteorological conditions over the area indicated in the built-in map of the DSS.

The interface of the DSS shown in Figure 2 allows to choose the area of flight, mission, type of unmanned aircraft, and flight parameters. The characteristics that correspond to particular UAS are indicated and then used by the system to assess the weather-related risks for general flight. The information about current weather conditions is automatically collected and indicated in the panel of the DSS. There is an option to switch panels to demonstrate the operative weather. It is proposed to be informed about the present state of the atmosphere using data from the sensors placed on the other unmanned aircraft that perform missions in the area of intended flight. The information from the unmanned aircraft that perform flight in the area indicated in Figure 2 is shown in Table 1. The red color covers

the forbidden flight zones. However, thanks to the technology of geo-zoning [17, 18] and the protection of sensitive areas, a route was modelled that demonstrates the effective execution of the UAV mission.

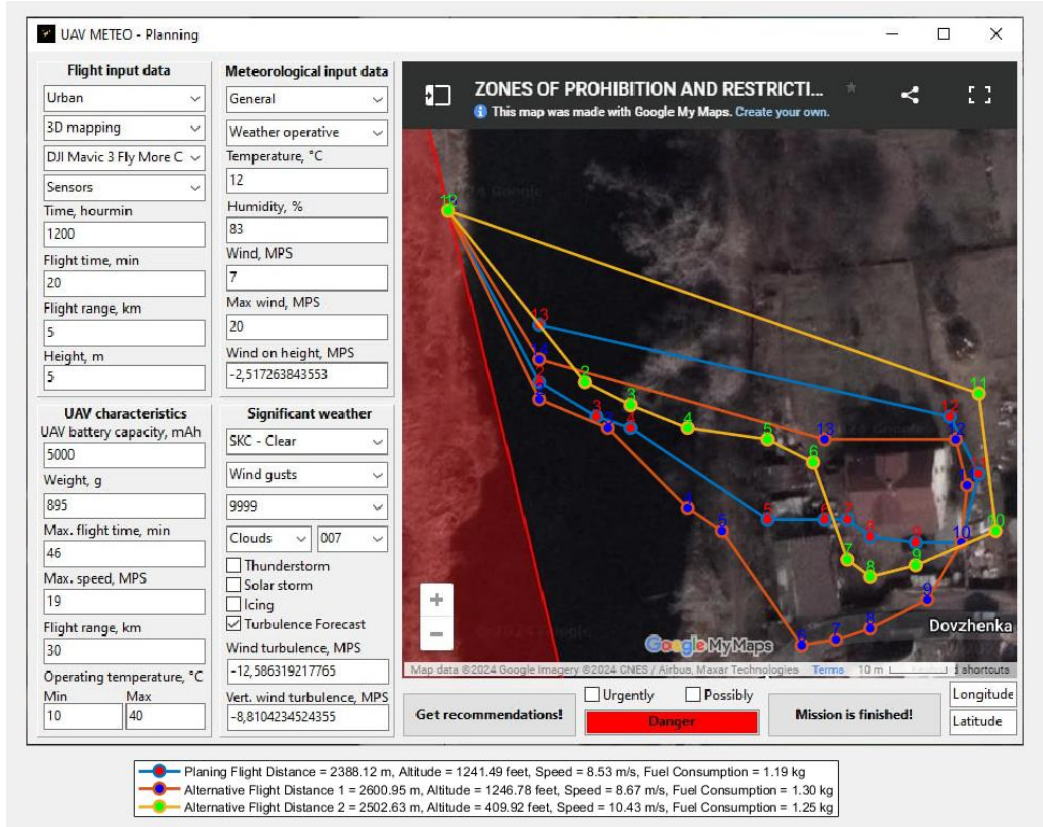


Figure 2: DSS interface and simulated trajectory options.

We can see from Figure 2 shows that the initial flight path passes through an area with buildings and the mission involves flying among these buildings. The blue trajectory shows the planned flight route that will allow the operator to fly and obtain photo/video data about the area. To calculate low-level turbulence, we use the Bellman-Fort model [19]. The model takes into account wind speed and the size of structures in the wind path. DSS identifies the flight as unsafe in the area near buildings and offers alternative flight options.

The planned flight trajectory is indicated with a blue line. The system identifies the flight in point 7 as dangerous because of increased wind and mechanical turbulence. This can be seen in Table 1. The two alternatives are proposed. In this particular simulation, the trajectory was corrected based on Bellman's algorithm [20, 21].

The total length of the route is calculated using the formula (1):

$$d = \sum_{i=1}^n \sqrt{(x_{i+1} - x_i)^2 + (y_{i+1} - y_i)^2 + (z_{i+1} - z_i)^2} \quad (1)$$

where $(x_{i+1} - x_i)$, $(y_{i+1} - y_i)$ and $(z_{i+1} - z_i)$ are the differences between the x, y and z coordinates of the neighboring points of the route; n is the number of selected control points on the route, which demonstrates the change of the UAV's heading.

The x and y coordinates form the foundational elements of the coordinate system, allowing precise tracking of the UAV's location within the designated flight sector. Here, the x coordinate represents latitude, determining the UAV's position in the North-South direction, while the y coordinate represents longitude, indicating the UAV's position in the east-west direction.

Table 1
Information from the drone

Point	Planning Flight Distance			Alternative Flight Distance 1			Alternative Flight Distance 2		
	Wind, m/s	Speed, m/s	Temp., °C	Wind, m/s	Speed, m/s	Temp., °C	Wind, m/s	Speed, m/s	Temp., °C
1	1.4	8.1	12	1.4	8.3	12	1.4	10.1	12
2	1.5	8.5	12.2	1.5	8.5	12.2	1.5	10.3	12.2
3	1.8	8.4	12.2	1.8	8.4	12.2	1.8	10.4	12.2
4	1.6	8.8	12.2	1.6	8.8	12.2	1.6	10.8	12.2
5	1.5	8.6	12.2	1.5	8.6	12.2	1.5	10.6	12.2
6	1.5	8.1	12.3	1.5	8.1	12.3	1.5	9.1	12.3
7	7	8.8	12.2	1.7	8.8	12.2	1.7	9.8	12.2
8	2	8.9	12.2	2	8	12.2	2	8.8	6.9
9	2.05	8.3	12.3	2.05	8	12.3	2	9.1	7
10	2.2	9.1	12.4	2.2	8.1	12.4	1.3	10.3	6.6
11	2	8.9	12	2	8	12	1	10.4	6.3
12	2	6.2	12.1	2	9	12.1	2	2.4	7
13	1.3	8.5	12.1	1.3	9.2	12.1	-	-	-
14	1	3.2	12.4	1.6	6.1	12.4	-	-	-
15	-	-	-	1.2	3.4	12.4	-	-	-

In addition to the horizontal positioning provided by the x and y coordinates, the coordinate system employed in UAV missions incorporates a crucial vertical dimension: the flight altitude. This vertical component is essential in aviation, as it not only ensures safe navigation but also allows for mission-specific adjustments based on terrain, obstacles, and airspace regulations.

In the software environment, it is implemented as a function that takes arrays of x and y coordinates of the route points and returns the total length of the route based on its trajectory in space [22, 23]. In the software environment, this formula is implemented as a function that takes each individual section of the route length as a separate full-fledged flight route, which demonstrates the uniqueness and peculiarity of the mission, which has other micro-missions.

The flight parameters for each of the options and intended flight trajectory are also shown in the lower part of the interface shown in Figure 1. This information can be used for

final decision-making depending on the chosen priorities [24, 25]. The flight parameters information and atmospheric conditions information are summarized in Table 1. Analyzing the flight parameters of the intended and proposed options it is possible to say that system recommendations allow performing flight operations despite the presence of weather-hazardous areas along flight trajectory with rather no marked loss in flight efficiency (fuel consumption, flight time, etc.).

3. Considerations on communication to share operative information

The presented system operation is based on operative meteorological information sharing between mobile participants of air traffic in U-space and stationary participants (remote pilots, control stations, flight controllers) [26]. Therefore, the consideration of modern technologies that can be used for weather data dissemination is an important task. We chose to analyze the ZigBee wireless technology [27] taking in mind the advantages of this protocol [28]: rather low cost and ability to connect a larger number of devices, security, and simplicity in implementation, reliability, and mesh topology when communication that give the possibility to organize communication between devices without central node.

For this purpose, the signal power was calculated with signal losses due to propagation in free space and other factors affecting its propagation. The distance from the transmitter to each point is calculated using the formula for the distance between two points in three-dimensional space. (0:0:0) is the origin of coordinates for considered area (1).

The signal power P_r at each point is calculated using a formula that includes distance loss, obstacle loss, and other losses:

$$P_d = P_t - (20 \log_{10} \left(\frac{d_{total} - d}{d_{total}} \right) + 20 \log_{10}(f) + 20 \log_{10} \left(\frac{4\pi}{c} \right)), \quad (2)$$

where $P_t = 160$ dBm for the example in Figure 3 is the transmitter power; $d_{total} = 96.0469$ m is the distance between the points of location of transmitter and the receiver; d from 0 m to 96.0469 m is the distance from the point to the receiver; $f = 2.4$ GHz is the frequency of the signal; $c = 3 \cdot 10^8$ is the speed of light.

The formula for calculating interference from Wi-Fi takes into account the influence of signals from other Wi-Fi routers on the ZigBee signal. Usually, this interference is taken into account as additional power loss due to interference:

$$PL_{Wi-Fi} = 10 \log_{10} \left(n_{routers} 10^{\left(\frac{20 \log_{10}(d_{router}) + 20 \log_{10}(f) + 20 \log_{10} \left(\frac{4\pi}{c} \right)}{10} \right)} \right), \quad (3)$$

where PL_{Wi-Fi} is the loss of power from interference from Wi-Fi; $n_{routers} = 20$ is the number of affected Wi-Fi routers; d_{router} from 0 m. to 96.0469 m. is the distance to the Wi-Fi router, which is taken into account in the calculations; $f = 2.4$ GHz is the frequency of the Wi-Fi signal; $c = 3 \cdot 10^8$ is the speed of light.

The average ZigBee signal loss per wall is determined experimentally depending on the material of the wall, its thickness, the presence of metal elements in the wall and other factors. Common practice is to use values between 3 and 6 dB for internal walls and up to

12 dB for external walls. Such values may vary. The variation depends on some specific conditions and features of the premises. We will use the largest average values

$$PL_{wall} = PL_{ext}n_{ext} + PL_{int}n_{int}, \quad (4)$$

where PL_{ext} up to 12 dB is the power loss from the external wall; $n_{ext}= 4$ is the number of external walls; PL_{int} values between 3 and 6 dB is the power loss from the internal wall; $n_{int}= 2$ is the number of internal walls.

If there is an initial signal power (P_t) to calculate power loss due to distance (P_d), power loss due to walls (PL_{wall}) and power loss due to Wi-Fi (PL_{Wi-Fi}), then total power loss (PL_{total}) can be calculated by formula:

$$PL_{total} = P_t - PL_{wall} - PL_{Wi-Fi} - P_d, \quad (5)$$

where PL_{total} is the total loss of signal power in decibels, which includes losses due to walls, Wi-Fi and distance.

This value indicates how much the signal power will be reduced from the transmitter to the receiver due to all these losses. The greater the value of PL_{total} is, the lower the signal power at the receiver will be. In Figure 3, the signal attenuation comparison between line-of-sight propagation and under the presence of buildings and Wi-Fi influence is shown.

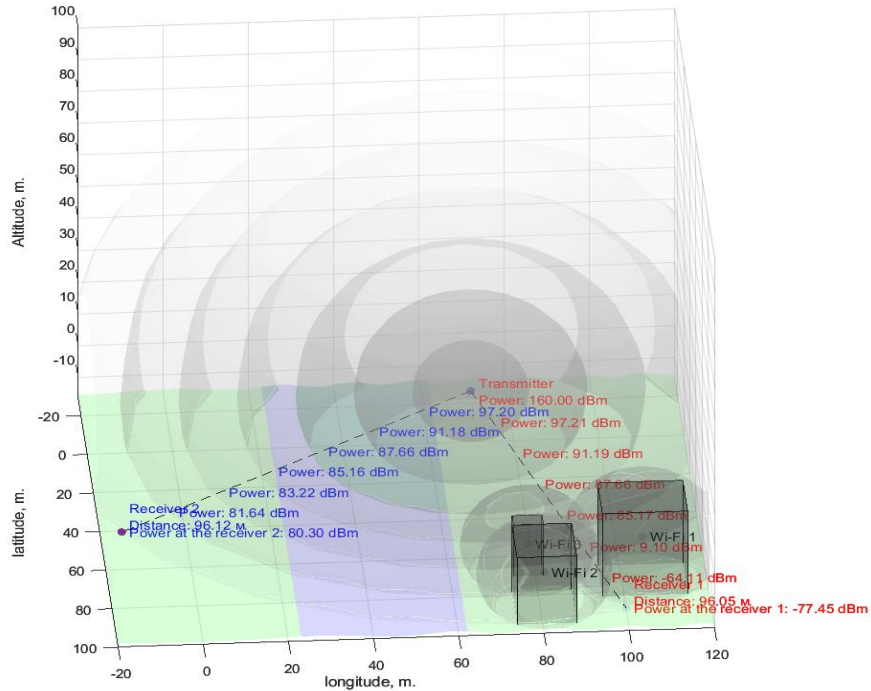


Figure 3: Comparison of ZigBee signal attenuation in line-of-sight and building obstacles and noise from Wi-Fi routers.

It is possible to see from Figure 3 that Zig Bee provides rather good communication in the line-of-sight conditions. We observe rather slight attenuation at a distance of 96 m. However significant influence is made by Wi-Fi routers. In this case, the relatively limited range for communication is provided when Zig-Bee technology is utilized. Therefore, the additional amplification of the signal is required.

There are also some restrictions connected with the use of ZigBee technology. These include the relatively limited range of communication. Therefore, it was our motivation to investigate the restriction and estimate the possibility of ZigBee technology for operative weather data sharing for decision support of UAS operators or automated flight trajectory correction.

4. Conclusions

In this paper, we considered and analyzed the operation of DSS which utilizes the distributed network of UASs to obtain operative information about weather-related hazards along the flight path. We presented the simulated example of DSS operation and options for operative flight path correction in urban environment. The simulation results demonstrate the consistency of the system to give recommendations concerning the planned mission, type of the unmanned aircraft and its characteristics, and planned area taking into account the geo-fencing and sensitive areas.

The system can be used by remote pilots or implemented as a component of the onboard flight control system for hazard detection and operative conflict resolution. The proposed method of obtaining information about present state of the atmosphere and considered system can be used as the basis for dynamic geo-fence implementation. The simulation of proposed trajectory corrections was done and discussed. Simulation results have shown the possibility of operative correction of UAS flight taking into account the mission, area, and type of aircraft. Therefore, different decisions can be proposed for different scenarios. Some discussions on the communications between distributed networks of air traffic participants were done.

5. Future Research

Future research will broaden the current study into the context of modern trends in urban planning. Such trends might include vertical farms, green and smart buildings. First, multistory vertical farms can create line-of-sight obstructions in addition to intense light emissions caused by artificial LED lighting. Thus, when facade glazing is used to enclose growing premises in such buildings, it is expected that it will cause a significant visual lightning obstacle for UAS.

Second, green roofs and facades are commonly used for vertical farms and many other types of buildings, which creates a significant vegetation area on the external walls and roofs. Such a type of surface can absorb, scatter, or reflect radio waves, causing signal degradation and distortion different from commonly used building materials.

Finally, smart buildings, including vertical farms, typically incorporate a wide range of IoT devices and sensors that collect data related to building management, indoor and outdoor environmental conditions. In turn, such information exchange could be beneficial for UAS-based smart city applications. Modern urban planning trends will be further studied to determine their influence on the choice of telecommunication technologies, data transmission protocols, information exchange, and possibilities of smart city implications.

References

- [1] F. Carippo, A. Fung, E. Hunt, V. Passo, Unmanned aircraft systems integration into European airspace and operation over populated areas, Final report, Research for TRAN Committee, 2023, pp 1–83. doi:10.2861/489361.
- [2] Commission Implementation Regulation (EU), 2024. URL: <https://eur-lex.europa.eu/legal-content/EN/TXT/?uri=CELEX%3A32019R0947>.
- [3] What is U-space?, 2024. URL: <https://www.easa.europa.eu/en/what-u-space>.
- [4] A.M. Rizwan, L.Y.C. Dennis, C. Liu, A review on the generation, determination and mitigation of Urban Heat Island, *Journal of Environmental Sciences* 20 (2008) 120–128.
- [5] K. Adkins, M. Akbas, M. Compere, Real-Time Urban Weather Observations for Urban Air Mobility, *International Journal of Aviation, Aeronautics, and Aerospace* 7(4) (2020) 11. doi: 10.15394/ijaaa.2020.1540.
- [6] P.D. Williams, Increased light, moderate, and severe clear-air turbulence in response to climate change, *Adv. Atmos. Sci.* 34(5) (2017) 576–586. doi:10.1007/s00376-017-6268-2.
- [7] E. Ranquist, M. Steiner, B. Argrow, Exploring the range of weather impacts on UAS operations, in: *Proceedings of the 18th Conference on Aviation, Range and Aerospace Meteorology*, AMS, United States, 2018, pp. 1–11. URL: https://ams.confex.com/ams/97Annual/webprogram/Manuscript/Paper309274/J3_1_Exploring_Range_of_Weather_Ranquist.pdf.
- [8] M. Rajawat, Weather conditions and its effect on UAS, *International Research Journal of Modernization in Engineering Technology and Science* 12(03) (2021) 1–7. URL: https://www.irjmets.com/uploadedfiles/paper/volume_3/issue_12_december_2021/17501/final/fin_irjmets1641191312.pdf.
- [9] P. James, S. Matthias, Weather Guidance for Unmanned Aircraft Systems, National Center for Atmospheric Research, 2017. URL: <https://ral.ucar.edu/aap/weather-guidance-for-unmanned-aircraft-systems-uas>.
- [10] Yu. Averyanova, E. Znakovskaja, Weather Hazards Analysis for small UASs Durability Enhancement, in: *Proceedings of the 6-th International Conference on Actual Problems of Unmanned Air Vehicles Developments, APUAVD*, IEEE, Ukraine, 2021, pp. 41–44. doi: 10.1109/APUAVD53804.2021.9615440.
- [11] R. Kashyap, Decision Support Systems in Aeronautics and Aerospace Industries. In T. Shmelova, et al., (Eds.), *Automated Systems in the Aviation and Aerospace Industries*, IGI Global, 2019, pp. 138–165. doi: 10.4018/978-1-5225-7709-6.ch005.
- [12] Y. Averyanova, Y. Znakovska, The Spatial Relationships of Meteorological Data for Unmanned Aerial System Decision-Making Support, in: *Proceedings of International Conference on the Electronic Governance with Emerging Technologies, Communications in Computer and Information Science*, vol 1666, Springer, Cham, 2022, pp. 64–80. doi:10.1007/978-3-031-22950-3_6.
- [13] Safety Management Manual, ICAO Doc 9859, 4th edition, ICAO, 2018. URL: <https://store.icao.int/en/safety-management-manual-doc-9859>.

- [14] Flight Safety Analysis Handbook, 2011. URL: https://www.faa.gov/about/office_org/headquarters_offices/ast/media/Flight_Safety_Analysis_Handbook_final_9_2011v1.pdf.
- [15] Y. Znakovska, Y. Averyanova, Simulation of UAS Operator's Decision-Making under Different Weather Conditions, in: Proceedings of the 4th International Conference on Modern Electrical and Energy System, MEES, IEEE, Kremenchuk, Ukraine, 2022, pp. 1–4. doi: 10.1109/MEES58014.2022.10005627.
- [16] Yu. Averyanova, Ye. Znakovska, Decision-making automation for UAS operators using operative meteorological information, in: Proceedings of the 1st International Workshop on Computer Information Technologies in Industry 4.0, CITI-2023, Ternopil, Ukraine, 2023, pp. 139–149. URL: <https://ceur-ws.org/Vol-3468/paper8.pdf>.
- [17] C. Boselli, J. Danis, S. McQueen, A. Breger, T. Jiang, D. Looze, D. Ni, Geo-fencing to secure airport perimeter against UAS, International Journal of Intelligent Unmanned Systems 5(4) (2017) 102–116. doi: 10.1108/IJIUS-02-2017-0002.
- [18] J.S. Kumar, S.K. Pandey, M.A. Zaveri, M. Choksi, Geo-fencing Technique in Unmanned Aerial Vehicles for Post Disaster Management in the Internet of Things, in: Proceedings of the Second International Conference on Advanced Computational and Communication Paradigms, ICACCP, Gangtok, India, 2019, pp. 1–6. doi: 10.1109/ICACCP.2019.8882934.
- [19] Fast Eddy Model, 2024. URL: <https://github.com/NCAR/FastEddy-model>.
- [20] Shortest Path: Dijkstra's and Bellman-Ford, 2024. URL: <https://courses.cs.duke.edu/spring18/compsci330/Notes/shortestpath.pdf>.
- [21] A.N. Rudiakova, Y.A. Averyanova, F.J. Yanovsky, Aircraft Trajectories Correction using Operative Meteorological Radar Information, in: Proceedings of the International Radar Symposium, 2020, pp. 256–259. doi: 10.23919/IRS48640.2020.9253799.
- [22] V. Larin, O. Solomentsev, M. Zaliskyi, A. Shcherban, Y. Averyanova, I. Ostroumov, N. Kuzmenko, O. Sushchenko, Y. Bezkorovainyi, Prediction of the final discharge of the UAV battery based on fuzzy logic estimation of information and influencing parameters, in: Proceedings of the 3rd KhPI Week on Advanced Technology (KhPIWeek), Kharkiv Ukraine, 2022, pp. 1–6. doi: 10.1109/KhPIWeek57572.2022.9916490.
- [23] I. Ostroumov, N. Kuzmenko, Y. Bezkorovainyi, Y. Averyanova, V. Larin, O. Sushchenko, M. Zaliskyi, O. Solomentsev, Relative navigation for vehicle formation movement, in: Proceedings of the 3rd KhPI Week on Advanced Technology (KhPIWeek), Kharkiv, Ukraine, 2022, pp. 1–4. doi: 10.1109/KhPIWeek57572.2022.9916414.
- [24] O. Sushchenko, Y. Bezkorovainyi, V. Golitsyn, N. Kuzmenko, Y. Averyanova, M. Zaliskyi, I. Ostroumov, V. Larin, O. Solomentsev, Integration of MEMS inertial and magnetic field sensors for tracking power lines, in: Proceedings of the XVIII International Conference on the Perspective Technologies and Methods in MEMS Design (MEMSTECH), 2022, Polyana, Ukraine, 2022, pp. 33–36. doi: 10.1109/MEMSTECH55132.2022.10002907.
- [25] O. Sushchenko, Y. Bezkorovainyi, O. Solomentsev, N. Kuzmenko, Y. Averyanova, M. Zaliskyi, I. Ostroumov, V. Larin, V. Golitsyn, Airborne sensor for measuring components of terrestrial magnetic field, in: Proceedings of Conference on Electronics and

Nanotechnology, Kyiv, Ukraine, 2022, pp. 687–691. doi: 10.1109/ELNANO54667.2022.9926760.

- [26] K. Dergachov, O. Havrylenko, V. Pavlikov, S. Zhyla, E. Tserne, V. Volosyuk, et al., GPS usage analysis for angular orientation practical tasks solving, in: Proceedings of IEEE 9th International Conference on Problems of Infocommunications, Science and Technology (PIC S&T), Kharkiv, Ukraine, 2022, pp. 187–192. doi: 10.1109/PICST57299.2022.10238629.
- [27] Introduction to ZigBee, 2024. URL: <https://www.geeksforgeeks.org/introduction-of-zigbee>.
- [28] A. Tatachar, Sh. Kondur, R. Amith, C. Varun, C. Kiran, K. V. Vishwas, Zigbee, It's Applications and Comparison with Other Short Range Network Technologies, International Journal of Engineering and Technical Research, 10 (2021) 891–897. doi: 10.17577/IJERTV10IS060412.